

Phase Unwrapping in Fringe Projection Systems Using Epipolar Geometry

Christian Bräuer-Burchardt, Christoph Munkelt, Matthias Heinze, Peter Kühmstedt,
and Gunther Notni

Fraunhofer IOF Jena,
Albert-Einstein-Str. 7, D-07745 Jena, Germany
christian.braeuer-burchardt@iof.fraunhofer.de

Abstract. A new method for phase unwrapping is introduced which realizes the unwrapping of phase images without binary codes produced by fringe projection systems using at least two cameras and one projector. The novelty of the method is the use of the epipolar geometry between the two cameras and the projector in order to achieve a unique point correspondence. The method is suited for systems which should realize a short recording time for the image sequence acquisition. It is very robust even at positions with abrupt change of depth.

Keywords: fringe projection, phase unwrapping, optical measurement systems, measuring accuracy, calibration, computer vision.

1 Introduction

Measuring systems using fringe projection are increasingly used in industrial, technical and medical applications. Whereas the demands concerning flexibility, measuring accuracy, amount of measurement data and fields of application always increase, the processing time should be reduced. On the one hand new developments in computer technology help to satisfy these demands but on the other hand new technologies and algorithms must be developed.

In order to realize a contactless determination of the surface of measuring objects several measuring principles have been established in the past decades. Methods using only photographs to reconstruct the 3D shape of measuring objects denoted by photogrammetry are confronted to methods using structured light. However, these principles have already been merged leading to methods called phasogrammetry or active stereo vision.

Methods using the projection of sinusoidal fringe patterns have to solve the problem of phase unwrapping. This can be realized e.g. by the use of multiple spatial frequencies [1], temporal phase unwrapping methods [2], or the use of Gray-Code sequences [3, 4]. Because of the unambiguousness the use of the Gray-Code leads to robust results. However, longer image sequences must be recorded which is not always desired.

The goal of our work was to establish a method which needs a minimal number of images in a sequence in order to make fast applications (real-time app.) possible.

Recently, a number of methods for phase unwrapping using structured light projection has been developed.

A method of phase unwrapping by projection of trapezoidal patterns is suggested by Malz [5]. Maas [6] describes a method which projects dot rasters of various density onto the measuring object in combination with a simultaneous image recording by four cameras. The epipolar geometry information is used to realize the point correspondences between the camera images.

A real-time coordinate measurement is suggested by Zhang [7] where the phase unwrapping is realized by determination and tracking of a marker.

Sansoni et al. [3] provide the analysis and correction of systematic errors in 3D vision methods using Gray-Code and phase determination.

An interesting method for phase unwrapping using at least two cameras is presented by Ishiyama [8]. Starting after calibration of the system at a certain point seen by the first camera all candidates of corresponding 3D points are drawn back to their image in the second camera. If the wrapped phase differs significantly, the candidate is rejected. Thus the number of possible correspondences is drastically reduced. Another suggestion for 3D measurement using a one projector one camera fringe projection system given by Ishiyama [9] uses the invariance of cross-ratio of perspective projection.

In order to select a methodology which is optimal for a certain application one should consider the given measuring conditions and restrictions as well as the requested accuracy of the measuring result. Here we introduce a new method which realizes a robust phase unwrapping based on two perpendicular fringe directions.

In this paper, no comparison of different methods will be performed but merely a suggestion for phase unwrapping without the use of Gray-Code sequences is given. This may be useful for applications where a short recording time of the image sequences is necessary. Such applications are for example reconstruction of living objects (e.g. face recognition) which can be without motion only for a short time and other measurement tasks which require real-time processing.

2 Measuring Principles

2.1 Fringe Projection and Active Vision

Fringe projection has been developed to an important tool in industrial and medical applications [10]. It is used to measure the surface geometry of complex objects. It became a well established method as well as photogrammetry and stereo imaging. Different methods have been developed in the past. The differences lie in the origin of the required measurement values for the calculation of the 3D data.

In principle, there are four different ways to obtain the measuring values for the calculation of the 3D co-ordinates using structured light: first, the classical approach of fringe projection, second, the uniform measurement scale method [11], third, the photogrammetry [12] and, fourth active stereo vision [13].

The classical approach of fringe projection can be outlined as follows. A fringe projection unit projects some well defined fringe sequences for phase calculation onto the object, which is observed by a camera. Measurement values are the phase values

(ϕ) as a result of the fringe projection and the corresponding image co-ordinates $[x_1, y_1]$ of the camera. The 3D co-ordinates X, Y, Z of the measurement point are calculated on the basis of more or less simplified triangulation (collinearity) equations [12, 14]. It should be pointed out that in all cases the calculated 3D co-ordinate is directly dependent (proportional) on the phase value (ϕ).

The fringe projection method of uniform measurement scale is based on the exclusive use of phase values for 3D co-ordinate calculation, where one has to use at least three phase values from fringe projection (ϕ_i) $i=1..n$ [11]. Here the camera has no influence to the measurement accuracy. But as well as the classical approach phase errors affect directly the accuracy of the 3D co-ordinate value.

Using the active vision method, images of the object are captured from two different perspectives. Pairs of image co-ordinates $[x_1, y_1]$ and $[x_2, y_2]$ resulting from the same object point (the homologous points) have to be identified. On the basis of these points the object can be reconstructed using triangulation methods. The basic task is to identify the homologous points in both cameras. In the case of active stereo vision a single intensity pattern or a sequence of patterns are projected onto the object under measure. To identify the homologous points in both cameras one has to use complex area [15] or image sequence based correlation techniques [16] using the captured intensity values. For example, the use of a sequence of statistical patterns was demonstrated for face scanning with the use of 20 patterns [17]. Commonly used area based correlation techniques are limited in the reachable precision caused by the deformation of the objects. Limits for this statistically correlation are the depth of sharpness (considerable smaller compared to fringe projection) and the spatial resolution.

We used a method, called “phase correlation” [4] that realizes a combination of phase measurement and stereo vision using image co-ordinates which is an enlargement of the method proposed by Thesing [18]. In this stereo based fringe projection approach we will use phase values as the starting point for the search of the homologous points.

2.2 Phase Unwrapping

The most robust method to achieve unambiguous phase values is the use of a binary code sequence, e.g. a Gray-Code sequence. Here, the phase values are completely unwrapped and the remaining task is to identify pairs of corresponding points in the two camera images. This is no real problem and is successfully performed in a number of measuring systems using fringe projection.

However, one aim is to reduce the number of images in the sequence in order to achieve a considerable shorter recording time. Hence, the Gray-Code sequence is omitted and the phase unwrapping must be realized without Gray-Code. In the literature a number of methods are described [1, 2, 19]. Our new method will be described in section 3. First, some other details of the methodology should be dealt with.

2.3 Phase Correlation

The basic set-up for a system using phase correlation consists of two cameras and one fringe projector (see Fig. 1). The principle of phase correlation (see also [4]) is to use the projected patterns only as virtual landmarks on the object to be measured and not

for the data calculation itself. The basic hardware for a phase correlation system consists of one fringe projector and two cameras. The projector generates two independent fringe sequences rotated by 90° to each other consisting of sinus and normally Gray-Code patterns. As a result we get two pairs of phase maps ($\phi_{1,x}$ $\phi_{1,y}$) and ($\phi_{2,x}$ $\phi_{2,y}$) at each object point M observed by the cameras from the different perspectives. Normally, these phase maps should be unwrapped where mainly the Gray-code technique is in use. These absolute phase maps can now be used for a point by point correlation between the images. The underlying procedure is shown in detail in Fig. 2.

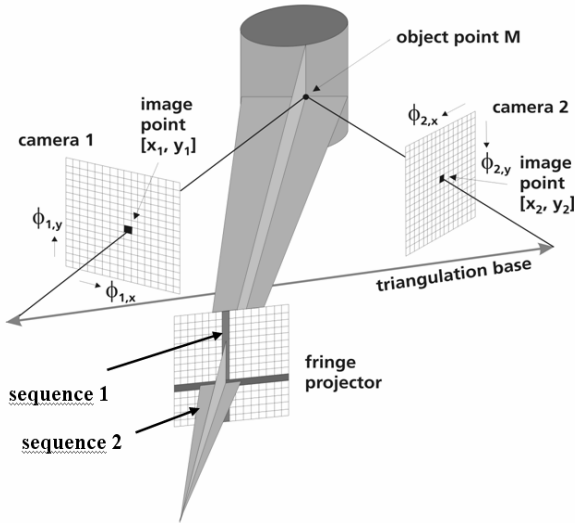


Fig. 1. Basic set-up for measurement using fringe projection with phase correlation

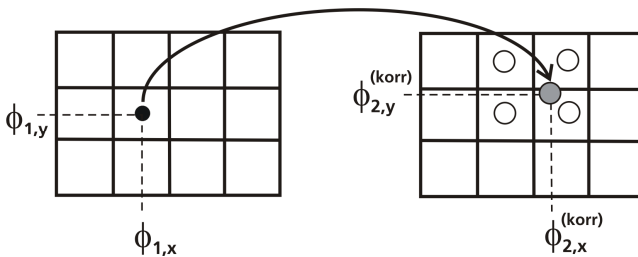


Fig. 2. Correlation of phase maps between two cameras

Starting from camera 1 with image co-ordinates $[x_1, y_1]$ and phase values ($\phi_{1,x}$, $\phi_{1,y}$) the corresponding image point in camera 2 is searched. Image co-ordinates $[x_2, y_2]$ in camera 2 are calculated with sub-pixel accuracy, based on the identical phase information (phase values ($\phi_{2,x}^{(korr)}$, $\phi_{2,y}^{(korr)}$) = ($\phi_{1,x}$, $\phi_{1,y}$)). The final results of this correlation are pairs of image points resulting from the same object point - the homologous

points. On the basis of the identified homologous points the calculation of the 3D coordinates is done by the well known triangulation (bundle adjustment) technique.

The complete process of the measurement process (data capturing and calculation) is outlined in detail as follows:

- Data capturing
 - Projection of two 90° rotated fringe sequences
 - Simultaneous image recording with both cameras
- Data calculation
 - Calculation of the phase maps for each camera
 - Point by point correlation of the phase maps between both cameras (→ homologous points)
 - Triangulation (co-ordinate calculation) between homologous points in both cameras
 - 3D shape of the measured object.

2.4 Epipolar Geometry

The use of the a-priori calibrated relative orientation between the two cameras leads to the so called epipolar geometry [14], well known in stereo vision, which identifies corresponding straight lines in the image planes of both cameras, see Fig. 3.

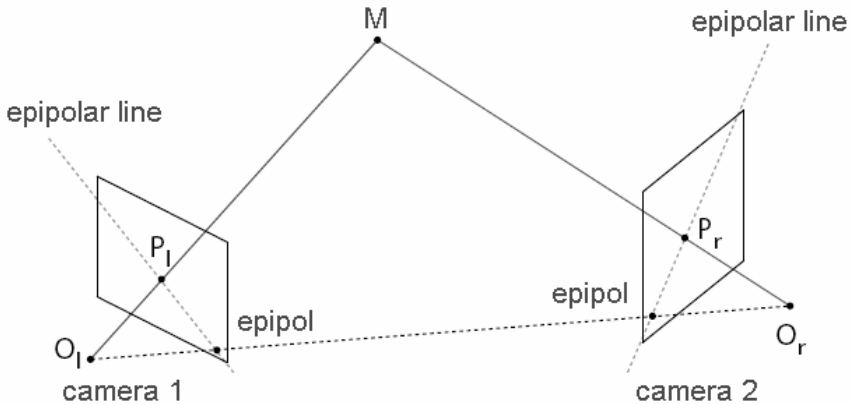


Fig. 3. Stereo camera arrangement – epipolar lines for a measurement point

3 The New Methodology

In the following, our new methodology to obtain 3D measurement data of the surface of the considered object will be described.

In a preprocessing step the measuring system including two cameras and one projector are calibrated (see [4]). These calibration data are used to determine the relative orientation between the two cameras and between each camera and the projector. It is assumed that the relative orientation does not change in the time of the measurement.

In the following the procedure of finding the point correspondences between the two camera images will be explained. The remaining part of 3D data calculation will be performed the same matter as usual, and its description is omitted here. The procedure will be described for one pair of corresponding points.

3.1 Finding Point Correspondences

This procedure will be applied to all points $p = (x,y)$ with co-ordinates x and y in the first image with a defined phase value $\phi(p) = \phi(x,y) = (\xi, \eta)$. Additionally, it can be applied in the reverse case, i.e. for all points in the second image.

First the two corresponding epipolar lines e_{12} and e_{21} defined by the orientation data and p are determined in the two camera images (see Fig. 4a and 4c). Considering the phase value of the points on e_{21} a number of say n correspondence candidates q_i , $i=1, \dots, n$ arise having a small phase difference

$$\Delta\phi_i = |\phi(p) - \phi(q_i)| = \sqrt{((\xi(p) - \xi(q_i))^2 + (\eta(p) - \eta(q_i))^2)} \quad (1)$$

with a value $\Delta\phi_i$ below a given threshold *thr*. However, the number n of candidates can drastically be reduced using the epipolar geometry between the cameras and the projector. See Fig. 4b for illustration. The regular grid points g_i are the unwrapped phase candidates in the projector image, i.e. all positions in the projector image plane producing the same phase value as the considered $\phi(p)$. Additionally, p defines together with the orientation data the corresponding epipolar lines e_{1p} and e_{p1} in the first camera image and the projector image, respectively. Thus the candidates for the corresponding point for p in the projector image are reduced to the intersections between e_{p1} and g_i leading to usually one or two remaining candidates c_j (see Fig. 4b). As well as before, the c_j define together with the orientation data two corresponding epipolar lines e_{p2} and e_{2p} in the projector image and camera 2 image, respectively. The intersection points q_i of e_{21} and e_{2p} are the final candidates for corresponding point for p . Usually only one candidate remains. If there is more than one intersection point q_i in the visible part of the image plane, all intersection points are stored. The final correspondence will be performed after complete processing using additional criterions described in the next section. See the example of Fig. 4. Although there are two candidates c_1 and c_2 in the projector image, there is only one visible intersection point q in the second camera image resulting in the correct corresponding point.

However, the geometrical situation may be so that often more than one candidate occurs, especially if there is no cant between the cameras and the projector. This should be considered in the mechanical design of the system. Systems which do not allow such a necessary cant should not be used together with this algorithm.

Despite of remaining errors in the epipolar geometry (e.g. by neglected distortion errors) the found point correspondences are erroneous and could be improved by the following post-processing step. Let the point correspondence between a point p from image 1 and a point q from image 2 be given. Then in a meaningful environment of q that point q' with minimal $\Delta\phi$ according to formula (1) is found as the corrected corresponding point to p .

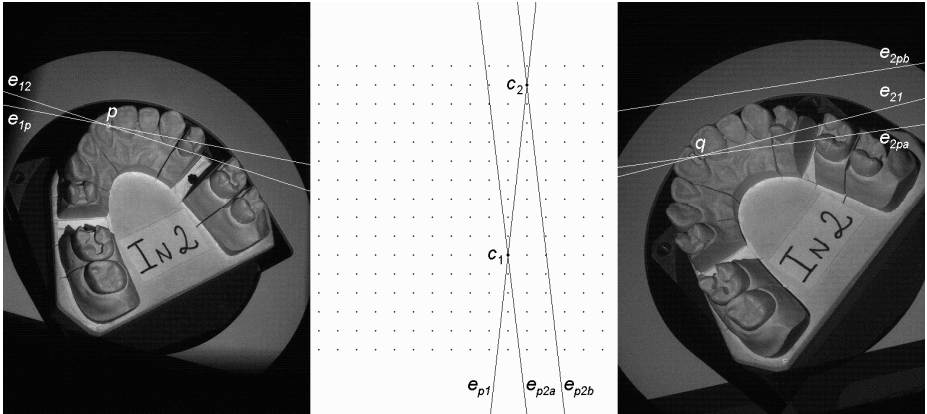


Fig. 4. Camera image 1 (left) with selected point p and two epipolar lines (e_{12} and e_{1p}), projector image (middle) with positions of phase values $\phi(p)$ (grid points), epipolar line e_{p1} and two epipolar lines e_{p2a} and e_{p2b} resulting from the two corresponding point candidates (c_1 and c_2), and camera image 2 (right) with epipolar line e_{21} and two epipolar lines e_{2pa} and e_{2pb} and one remaining intersection point q

3.2 Resolution of the Remaining Ambiguities and Correction of False Correspondences

False correspondences. Usually a number of correspondences will be erroneous. Especially points in the camera 1 image which do not have a corresponding point in image 2 (because of occlusions or different image contents) may produce a false positive correspondence within the search algorithm.

Initially, all points having exactly one correspondence are assumed to be correct. These correspondences produce a disparity map between the two camera images. By fitting a disparity plane d to all disparities, all disparity values have a difference $diff$ to the plane d . This difference should be in a meaningful range r which can be estimated using a disparity histogram. All correspondences outside r are rejected.

Additionally, the disparity gradient can be used to reject false point correspondences. This will be done with isolated points with a considerable disparity gradient to all of his neighbors having a one-to-one assignment.

Resolving ambiguities. If at least two candidates are present which were not rejected by the disparity plane difference the candidate with the highest probability will be selected.

If the candidate's co-ordinates are outside in the visible part of the image plane it will be rejected (probability = 0). The probability is now defined as the inverse difference of the disparity gradient concerning the unique point assignments in the environment of the point.

In order to determine the disparity gradient the epipolar geometry between camera 1 and camera 2 are used. The area of interest in the two images is covered by a meaningful band of corresponding epipolar lines. A disparity map of the unique point correspondences (which are assumed to be correct) is produced. By fitting a plane to

these disparities, a disparity plane is obtained. Correct correspondences should be near that plane and false correspondences should be far away. For the ambiguous points the disparity of all candidates is determined. The candidate with the smallest disparity difference to the disparity plane is selected. See the example of Fig. 5.

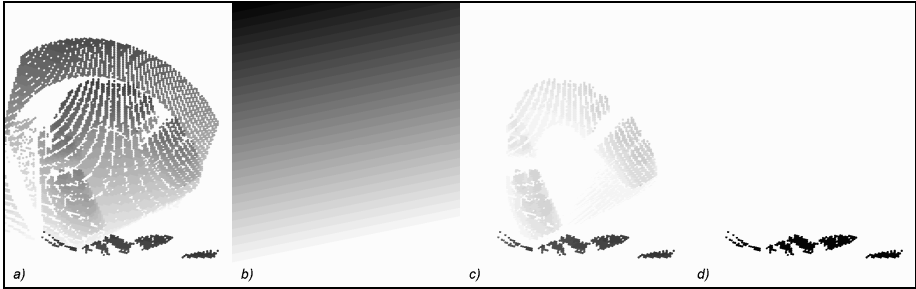


Fig. 5. Resolving ambiguities using disparity maps. From left to right: (grey value coded) disparity of representative points (a), fitted disparity plane (b), difference image (c) between (a) and (b), ambiguous points found by a binary threshold (d).

Additionally, the monotony of the co-ordinates along corresponding epipolar lines may be used. Because monotony is necessary here, it may be enforced. Not monotone regions must be rejected.

4 Experiments and Results

The new methodology was tested in a number of measurements using the measuring device “kolibri-flex 80” [4] at Fraunhofer IOF Jena, and the results were compared to those obtained by conventional measurement using Gray-Code sequences.

In order to evaluate the algorithm the following series of experiments was performed. A sequence of image recordings with projected fringes was produced and stored. These stored data were used to perform a self calibration of the system to obtain the necessary calibration data. Then one position of the sensor was selected and the stereo image pair from this position was produced. Using the Gray-Code sequence a reference data set producing the point correspondence was generated. A point cloud of 3D-points was generated using this dataset of point correspondences and displayed using a special software tool in order to evaluate the correctness of the point correspondences. If all correspondences seem to be correct, the reference dataset is complete. It determines the maximal number of correct point correspondences which can be produced using the new algorithm without using the Gray-Code sequence.

Now, the image sequences are used to produce unwrapped phase image pairs. Here the width of the projected fringes can also be manipulated and will be used as the parameter of the algorithm.

All in all ten image pairs were analyzed. As the result of the analysis the following quantities are determined: number of correct point correspondences before and after

Table 1. Results of point correspondence determination

Fringe width (pixel)	Found correspondences	Initially correct correspondences	Correct correspondences after resolving ambiguities
16	97	53	78
32	98	90	97
64	99	96	98
128	99.5	99	99
1024 (with Gray-Code)	99.5	99	99

resolving ambiguities. All results are given as percentage mean value over all analyzed image pairs. The results for sequence 1 are presented by Table 1.

It can be seen that the wider the fringes the higher is the number of initially found correct correspondences. However, one should be aware that the wider the fringes the higher the noise of the phase values. Thus the fringe width should be selected in such a way, that it becomes minimal with satisfying correspondence result. In our example 32 seems to be the best choice. Here false correspondences are minimal and hence the completeness is almost perfect. The noise of the resulting 3D surface data is the same as using the Gray-Code sequence. With a width of 128 the same result concerning completeness is obtained as with the use of Gray-Code, but the noise of the calculated 3D measurement data is higher by a factor of about two, because the standard fringe width of the rough phase in the reference measurement using the Gray-Code sequence was 32.

However, the optimal fringe width may depend also on other properties of the system, e.g. the orientation of the projector concerning the cameras. Consequently, in order to find the optimal configuration, additional experiments should be performed.

5 Summary, Discussion, and Outlook

A robust algorithm for phase unwrapping in fringe projection systems using epipolar geometry was introduced. It was shown that Gray-Code sequences may be omitted in order to achieve a faster image sequence recording. This may be interesting for high speed applications, e.g. in handheld 3D measurement systems. Of course, additional calculation effort is necessary. But designing fast calculation routines and using powerful computer technique this should be no restriction of a fast speed application.

In principle, the use of the projector orientation is not essential to solve the problem of phase unwrapping using two perpendicular projection directions because the second direction (eta-phase) may reduce the point correspondence candidates drastically, too. However, the position of the epipolar lines can not be detected with the same accuracy as the phase values. That means that errors may occur. If the change of eta-phase along the epipolar line is low, it is more difficult to identify correct correspondences without the projector information. Additionally, the shape of the measuring object influences the phase value profile along the epipolar line in the camera

images. Contrary, it does not in the projector image (see middle image of Fig. 4) which means an advantage of the use of the projector orientation.

Future work should include the following aspects: implementation of the algorithm into several measuring systems for 3D surface measurement using fringe projection, performing more experiments to evaluate the algorithm, comparing experimental results with those obtained without using the projector orientation concerning completeness, robustness and calculation time.

References

1. Li, E.B., Peng, X., Xi, J., Chicaro, J.F., Yao, J.Q., Zhang, D.W.: Multi-frequency and multiple phase-shift sinusoidal fringe projection for 3D profilometry. *Optics Express* 13, 1561–1569 (2005)
2. Zhang, H., Lalor, M.J., Burton, D.R.: Spatiotemporal phase unwrapping for the measurement of discontinuous objects in dynamic fringe-projection phase-shifting profilometry. *Applied Optics* 38, 3534–3541 (1999)
3. Sansoni, G., Carocci, M., Rodella, R.: Three-Dimensional Vision Based on a Combination of Gray-Code and Phase-Shift Light Projection: Analysis and Compensation of the Systematic Errors. *Applied Optics* 38(31), 6565–6573 (1999)
4. Kühmstedt, P., Munkelt, C., Heinze, M., Himmelreich, M., Bräuer-Burchardt, C., Notni, G.: 3D shape measurement with phase correlation based fringe projection. In: *Proc. SPIE*, vol. 6616, pp. B-1-B-9 (2007)
5. Malz, R.: Adaptive light encoding for 3-D sensing with maximum measurement efficiency. In: *Proc. 11th DAGM-symposium Hamburg 1986. Informatik-Fachberichte*, vol. 219. Springer, Heidelberg (1989)
6. Maas, H.-G.: Robust Automatic Surface Reconstruction with Structured Light. In: *IAPRS*, vol. XXIX, Part B5, pp. 709–713 (1992)
7. Zhang, S., Yau, S.T.: High-resolution, real-time 3D absolute coordinate measurement based on a phase-shifting method. *Optics Express* 14(7), 2644–2649 (2006)
8. Ishiyama, R., Okatani, T., Deguchi, K.: Precise 3-d measurement using uncalibrated pattern projection. In: *Proc. IEEE Int. Conf. on Image Proc (ICIP 2007)*, vol. 1, pp. 225–228 (2007)
9. Ishiyama, R., Sakamoto, S., Tajima, J., Okatani, T., Deguchi, K.: Absolute phase measurements using geometric constraints between multiple cameras and projectors. *Applied Optics* 46(17), 3528–3538 (2007)
10. Chen, F., Brown, G.M.: Overview of three-dimensional shape measurement using optical methods. *Opt. Eng.* 39, 10–22 (2000)
11. Kowarschik, R., Kühmstedt, P., Notni, G., Schreiber, W.: 3-coordinate measurement with structured light. In: *Proc. SPIE*, vol. 2342, pp. 41–49 (1994)
12. Schreiber, W., Notni, G.: Theory and arrangements of self-calibrating whole-body three-dimensional measurement systems using fringe projection technique. *Opt. Eng.* 39, 159–169 (2000)
13. Scharstein, D., Szeliski, R.: High-Accuracy Stereo Depth Maps Using Structured Light. *CVPR 2003*(1), 195–202 (2003)
14. Luhmann, T., Robson, S., Kyle, S., Harley, I.: *Close range photogrammetry*. Wiley-Interscience Publishing, Chichester (2006)
15. Robin, E., Valle, V.: Phase Demodulation from a Single Fringe Pattern Based on a Correlation Technique. *Appl. Opt.* 43, 4355–4361 (2004)

16. Albrecht, P., Michaelis, B.: Improvement of the spatial resolution of an optical 3-D measurement procedure. In: IEEE Instr. and Measurement Technology Conference (IMTC 1997), Ottawa (1997)
17. Wiegmann, A., Wagner, H., Kowarschik, R.: Human face measurement by projecting bandlimited random patterns. *Optics Express* 14(17), 7692–7698 (2006)
18. Thesing, J.: New approaches for phase determination. In: Proc. SPIE, vol. 3478, pp. 133–141 (1998)
19. Su, W.-H., Liu, H.: Calibration based two-frequency projected fringe profilometry: a robust, accurate, and single-shot measurement for objects with large depth discontinuities. *Optics Express* 14, 9178–9187 (2006)